J Bionic Eng 15 (2018) 443–451
DOI: https://doi.org/10.1007/s42235-018-0035-7

Journal of Bionic Engineering
http://www.springer.com/journal/42235

Finite Element Analysis of the Pelvis after Customized Prosthesis Reconstruction

Enchun Dong[1], Ling Wang[1*], Taimoor Iqbal[1], Dichen Li[1], Yaxiong Liu[1], Jiankang He[1], Binghui Zhao[2], Yuan Li[2]

1. *State Key Laboratory for Manufacturing System Engineering*, *Xi'an Jiaotong University*, *Xi'an* 710054, *China*
2. *Tianjin Medical Device Supervision and Testing Center*, *Tianjin* 300384, *China*

Abstract

Custom-made pelvic prostheses are normally employed to reconstruct the biomechanics of the pelvis for improving patient's life quality. However, due to the large demand of biomechanical performance around the pelvic system, the customized prosthesis needs to be studied for its strength and stability. A hemi-pelvic finite element model, including a custom-made prosthesis and the surrounded main ligaments, was created to study the strength and stability of the system. Based on the developed finite element model, the relationship between the pre-stress of the screws and the biomechanical performance of the reconstructed pelvis was investigated. Results indicate that the pre-stress should not exceed 1000 N during surgery in order to prevent fatigue fractures from happening to screws. Moreover, four screws were removed from the pelvic system without affecting the fixing stability of the system, which provide surgical guidance for surgeons in terms of safety and fixation.

Keywords: customized hemi-pelvic prosthesis, finite element analysis, biomechanics, screws pre-stress

1 Introduction

The pelvis is one of the most important structures in the human body, contributing to the stability and protection of the inner organs[1]. Among the three components of the pelvis, the ilium is the most frequently affected by tumors, and is therefore a common site for reconstruction[2]. Pelvic reconstruction after large resection remains a challenge in surgery owing to its complex anatomical structure.

Pelvic prosthesis is the primary means of pelvic reconstruction after an internal hemipelvectomy[3]. There are many types of pelvic prostheses such as modular pelvic prostheses[4,5], saddle prostheses[6,7], pedestal cups[8], and custom-made pelvic prosthesis[9,10]. Among them, custom-made prostheses can provide a better match with the patient's residual bone tissue[11], which in turn can reduce the risk of infection, chance of dislocation, or failure of the implant[10]. Therefore, custom-made prostheses are increasingly used nowadays.

Owing to their complex structure, studies on the biomechanics of the pelvis are quite rare. It is difficult to assess the stress or strain distribution throughout an entire reconstructed pelvis using simplified mathematical models or implanted prostheses, or experimentally using cadaveric tissue[12]. However, the Finite Element (FE) method has intrinsic advantages of restricting individual differences without the need for equipment or environmental variations[13]. It can be customized to the specific patient by gathering the geometric and material properties from the subject's own Computer Tomographic (CT) or Magnetic Resonance (MR) images[14]. Thus, the FE method is becoming increasingly popular in pelvic biomechanics research and is playing a critical role in a failure analysis and revised prosthesis designs[1,5,15–17]. Although some FE studies on custom-made prostheses have been carried out, studies on the influence of the pre-stress of the screws on the biomechanical performance of a Reconstructed Pelvis (RP) are rarely reported.

The aim of this study was to investigate the relationship between the pre-stress of the screws and the biomechanical performance of an RP. For this purpose, a

***Corresponding author:** Ling Wang
E-mail: menlwang@mail.xjtu.edu.cn

hemi-pelvic FE model, including a custom-made prosthesis and the main ligaments, was created from the CT scanning data of the patient. The stress distribution of the RP under different pre-stress situations was investigated. The maximum pre-stress of the screws was determined based on the fatigue strength of titanium alloy. Moreover, four screws on the alar part of the implant were removed and the stress distribution of the RP under different pre-stress situations was also calculated.

2 Materials and methods

2.1 Clinical information

A 64-year-old male patient, 168 cm in height and 68 kg in weight, was referred to the outpatient service of the People's Hospital of Inner Mongolia due to a left pelvic tumor. A customized prosthesis was implanted into the patient with 14 screws to reconstruct the patient's pelvis. According to the clinical records, the patient passed away six months after surgery, with no sign of infection or implant loosening. The patient's CT images were obtained before surgery with the permission from the ethics committee of hospital. Based on these CT images, a three-dimensional (3D) model of the pelvis was reconstructed, and a Finite Element Analysis (FEA) was carried out to determine the effects of pre-stresses of the screws on the performance of the pelvic prosthesis.

2.2 3D solid modeling

The CT images were imported into Mimics 16.0 (Materialise, Belgium) to construct triangle-based surface models of the sacrum, and the right and left ilia. These surface models were imported into Geomagic Studio 2012 (Geomagic, USA) for refinement and creation of the solid 3D models. These solid 3D models were then imported into UG 11.0 (Siemens PLM, USA) for error checking, and screws were then added into the installation holes of the implant. These screws were simplified as cylinders to facilitate the FEA applied at a later stage. The custom-made prosthesis was designed and manufactured based on the instructions of a surgeon. Finally, the solid 3D model of the RP was obtained. However, the patient's Normal Pelvis (NP) cannot be obtained directly because the left ilium was affected by tumor. Therefore, the NP was reconstructed through the mirror image of the healthy ilium onto the left side in Mimics. Then the same processes described above were used to generate the 3D model of the NP.

2.3 FEA model

Owing to their complex structure, four-node linear tetrahedron elements (C3D4) were chosen for the bones and implant, and were meshed using Hypermesh 14.0 (Altair, USA). For better accuracy, the screws were meshed by using the C3D8I (8-node linear elements, incompatible modes) in Abaqus/CAE (6.14, Dassault, France).

According to previous research regarding the relationship between Hounsfield units and bone density, as well as the relationship between bone density and Young's modulus, the pelvic materials were assigned using Mimics software based on the different grey values ($H.U$) using the following relations[18]:

$$\rho = 0.00069141 \times H.U + 1.026716, \tag{1}$$

$$E = 2017.3\rho^{2.46}. \tag{2}$$

The implant was fabricated using Selective Laser Melting (SLM) technology, and the equipment is EOSINT M280 (EOS Germany). The material applied was Ti-6Al-4V powder with particle size ranged from 15 μm to 53 μm. The material of the screws was also defined as titanium alloy. All materials used in this study are listed in Table 1.

The interfaces between the sacrum and ilia were tied because the bones of elderly persons are fused at these locations[19]. Friction occurred at the contact points between the implant and bones, with a friction coefficient of 0.1[20]. Tie constraints were used between the screws and bones to simulate a screw-thread fit. Tie constraints were also used between the implant and screws.

According to a study by Hao *et al.*[21], the major pelvic ligaments were simulated using spring elements

Table 1 Material properties used in present study

Component	Materials	Young's modulus (GPa)	Poisson's ratio
Left ilium	–	2.07 – 9.89	0.3
Sacrum	–	1.95 – 8.84	0.3
Right ilium	–	2.04 – 9.62	0.3
Implant	Titanium alloy	110	0.3
Screws	Titanium alloy	110	0.3

in Abaqus with a constant stiffness. The parameters of these spring elements are provided in Table 2. The sacrotuberous, sacrospinous, pubic, and iliolumbar ligaments were excluded on left side of the RP model because of the wide resection on the left side of the pelvis[10].

A vertical load of 810 N (1.2-times the body weight) on the S1 vertebra was applied (Fig. 1) without considering the muscular forces, which are negligible in a pelvis model according to a study by Dalstra *et al.*[22]. In addition, a bolt load was applied on the surface below the nut to simulate the pre-stress of the screw. In this case, the relationship between this pre-stress and the biomechanical performance of the RP can be analyzed by applying different pre-stress levels.

Table 2 Parameters of the spring elements

Ligament	Stiffness ($N \cdot mm^{-1}$)	Number of springs
Sacroiliac	5000	45
Sacrospinous	1500	12
Sacrotuberous	1500	30
Iliolumbar	1000	10
Superior pubic	500	10
Arcuate pubic	500	15

In this paper, three static conditions of the pelvis were calculated, *i.e.*, a two-leg stance, a healthy leg (right side), stance, and an injured leg (left side) stance. The nodes on both acetabulum cups were constrained to within five degrees of freedom (with the exception of a horizontal translation) for the two-leg stance, whereas the nodes on left and right cups were fully constrained within all degrees of freedom for the left and right leg stance, respectively[10] (Fig. 1).

The mesh sensitivity was investigated, and a mesh size of 2 mm was found to be sufficiently accurate because the relative error between mesh sizes of 2 mm and 1.5 mm was below 5%. The number of elements for the right ilium, sacrum, left ilium, implant, and screws was 66943, 33043, 84389, 52686, and 21731, respectively.

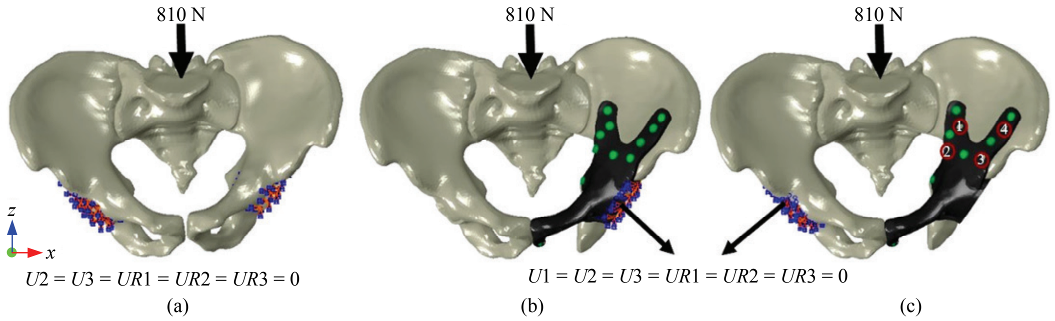

Fig. 1 Loading and boundary conditions. (a) Two-leg stance; (b) unhealthy leg stance; (c) healthy leg stance (with four screws removed).

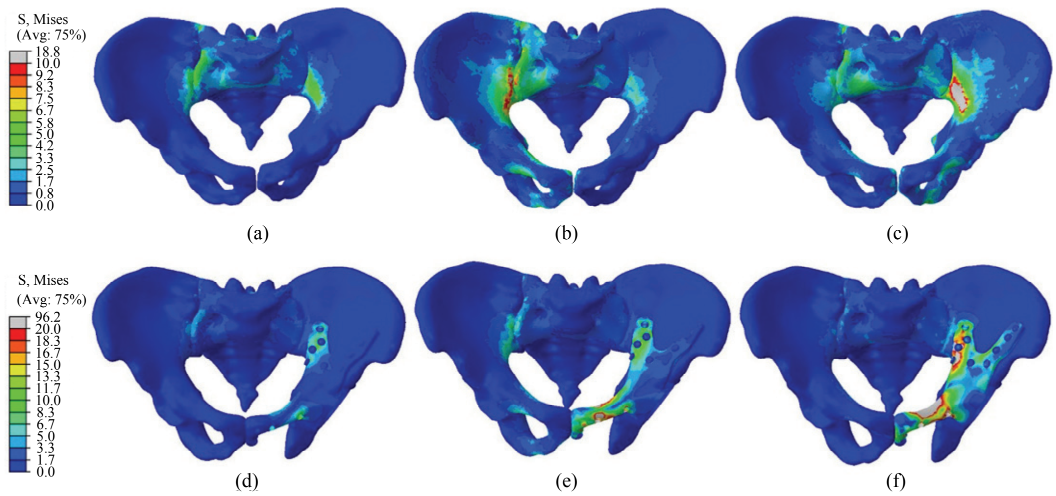

Fig. 2 Von Mises stress distribution of normal pelvis during (a) two-leg stance; (b) right leg stance; (c) left leg stance, and reconstructed pelvic during (d) two-leg stance, (e) healthy leg stance, and (f) unhealthy leg stance.

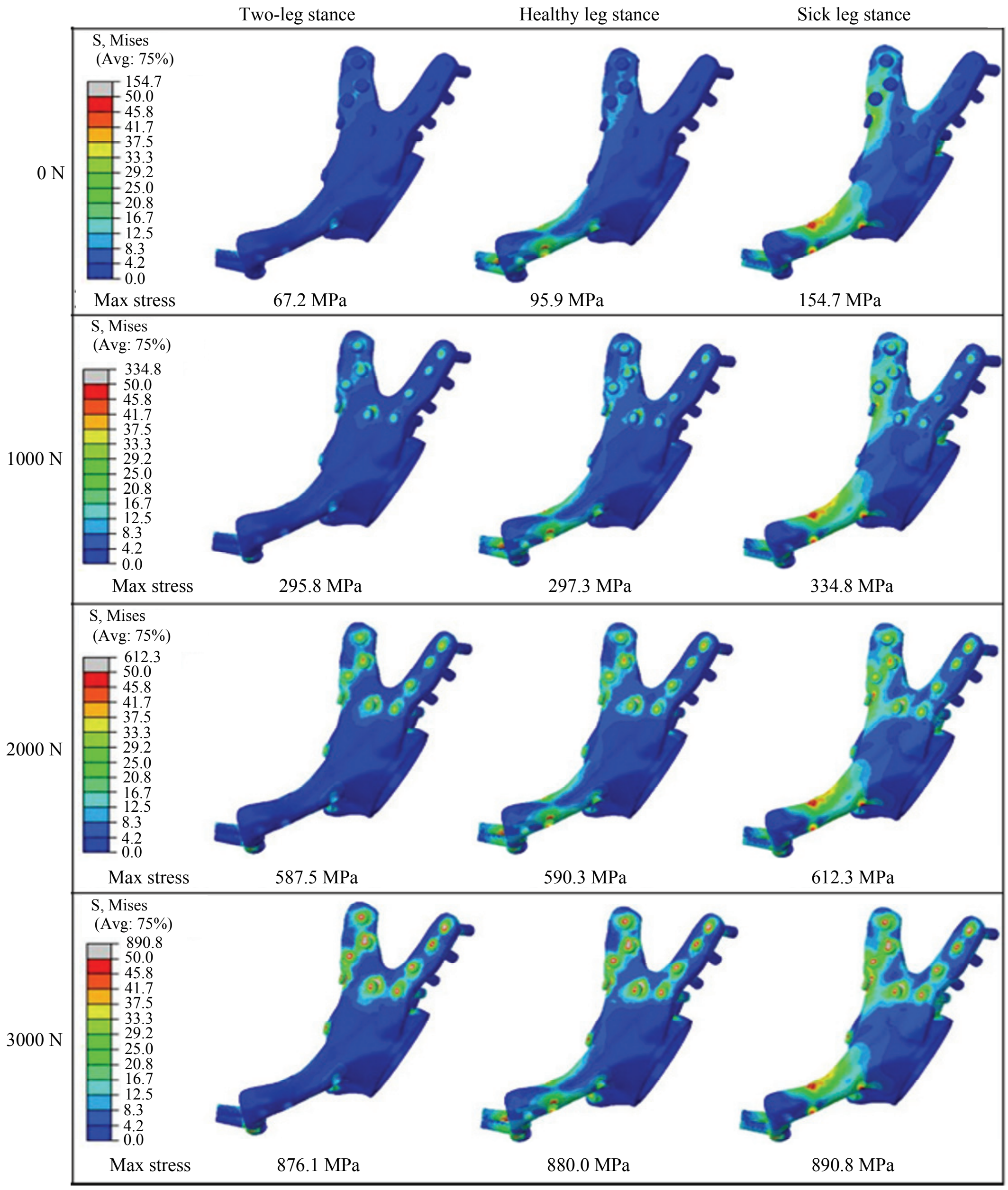

Fig. 3 Von Mises stress distribution under different pre-stresses (with all screws).

3 Results

3.1 NP analysis

The maximum von Mises stress for the two-leg stance, right-leg stance, and left-leg stance of the NP model was 8.0 MPa, 13.7 MPa, and 18.8 MPa, respectively, and the stresses were mainly distributed at the sacroiliac joint for the above three-mentioned conditions. Because of the stress shielding, the stresses were mainly distributed at the alar part and pecten pubis of the implant for the RP (Fig. 2).

3.2 RP analysis (with all screws)

The stress distribution of the RP under different pre-stress situations was calculated. It can be seen that the stress gathered and spread around the screws as the pre-stress increased (Fig. 3).

When the pre-stress was zero, the maximum von Mises stress was 5.9 MPa for the bone model, 67.2 MPa for the implant and 61.7 MPa for the screws for the two-leg stance situation. However, for a healthy leg stance and an unhealthy leg stance, the maximum von Mises stress of 9.7 MPa, 83.7 MPa, 95.9 MPa, and

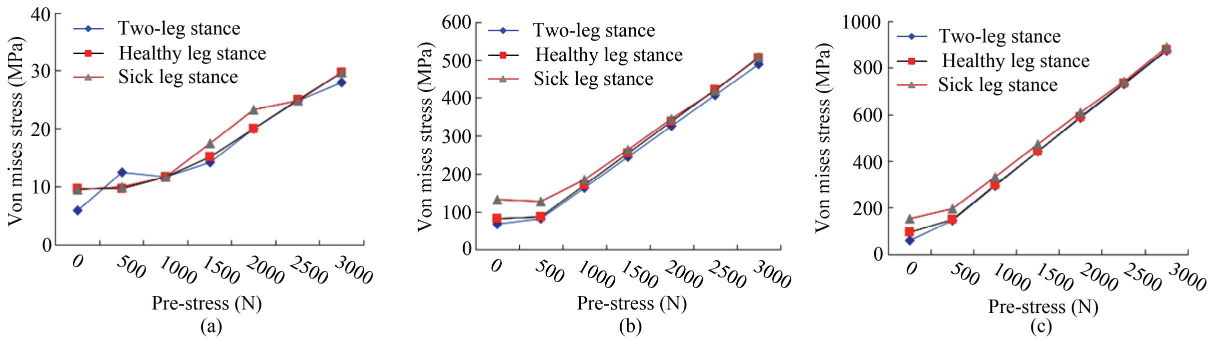

Fig. 4 Maximum von Mises stresses in (a) bone, (b) implant, and (c) screws under different pre-stresses (with all screws).

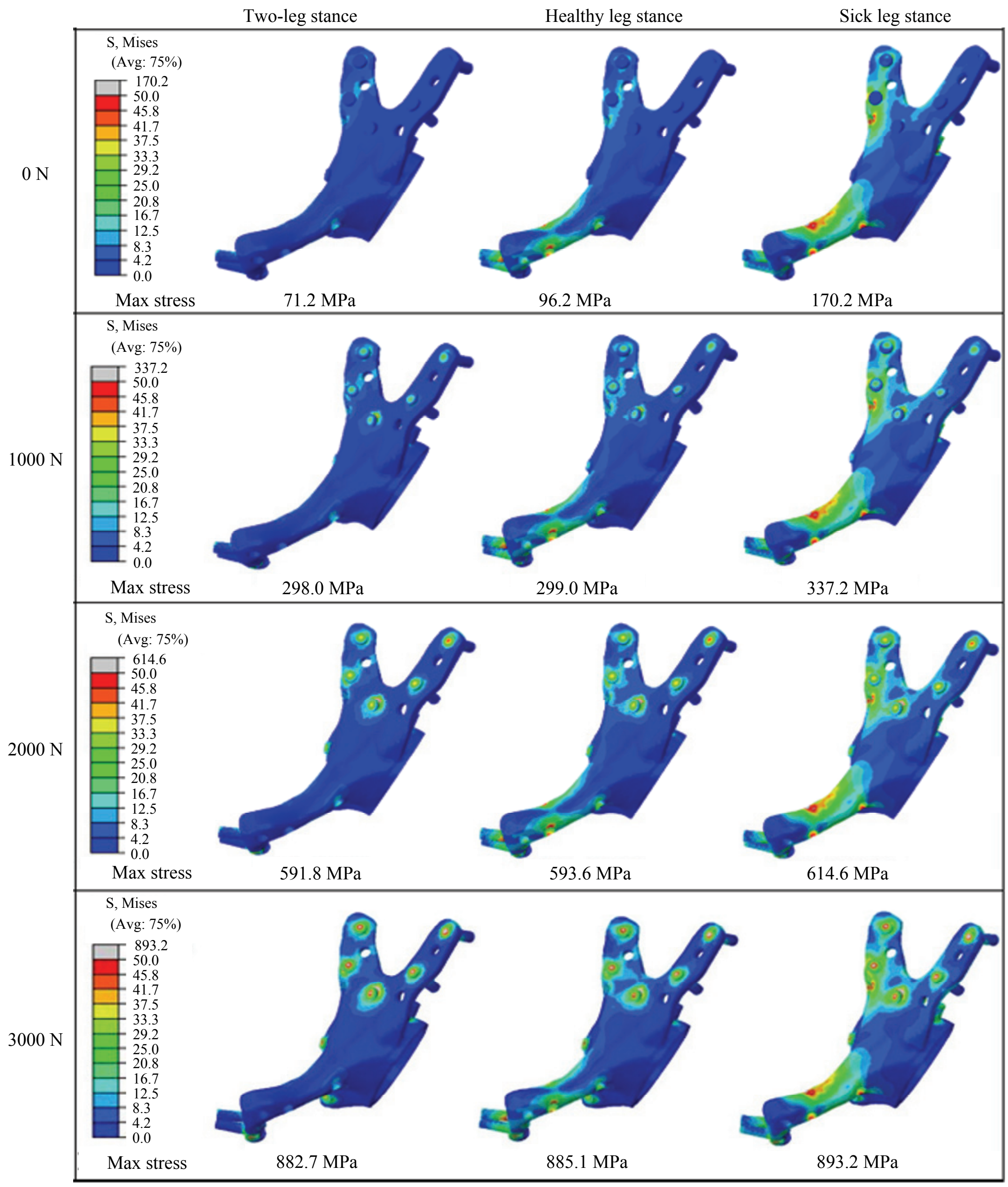

Fig. 5 Von Mises stress distribution under different pre-stresses (four screws removed).

9.5 MPa, 132.0 MPa, and 154.7 MPa was observed at these three parts, respectively. The maximum von Mises stresses in the bone, implant, and screws were quite different when the pre-stress was small (below 500 N); after that, the maximum von Mises stresses were increased approximately linearly with an increase in the pre-stress (Fig. 4). Moreover, in nearly all occurrences, the maximum stress of the screws was bigger than the maximum stress of the implant, and the maximum stress of the implant was bigger than the maximum stress of the bone.

3.3 RP analysis (four screws removed)

The stress distribution on the implant and screws was calculated with four screws removed from the RP system, and the results were shown in Fig. 5. With the exception of those positions where the screws were removed, the stress distribution results (after removing four screws, shown in Fig. 5) are basically the same as the results shown in Fig. 3.

After removing four screws, when the pre-stress was zero, the maximum stress was 5.9 MPa for bone part, 71.2 MPa for the implant and 71.0 MPa for the screws for the two-leg stance situation, whereas for a healthy or unhealthy leg stance, a maximum stress of 9.8 MPa, 90.0 MPa, and 96.2 MPa and 10.4 MPa, 156.7 MPa, and 170.2 MPa was observed for these three parts, respectively. The results of the maximum von Mises stress under different pre-stress situations are shown in Fig. 6. Compared to the results of the RP model with all screws (Fig. 4), the magnitude and variation of the stresses shown in Fig. 6 are quite similar.

3.4 Comparison of NP and RP

To compare the stress distribution between the NP and RP models, 11 points on the pelvic ring were selected, and the stresses at these selected points are summarized in Fig. 7. For the RP, the stresses of the selected points were measured under a pre-stress of 1000 N.

4 Discussion

In this article, a RP FE model was developed and the relationship between the pre-stress of screws and the biomechanical performance of an RP was investigated. On basis of the RP model, four screws were removed and the effects of fixation types of the implant on the performance of the RP were investigated.

When the pre-stress was zero, the highest von Mises stress was observed during the injured leg stance, and the peak stress of this stance is 20% – 40% larger than the peak stress of a healthy leg stance, and approximately 1.5- to 2-times greater than the peak stress of a two-leg stance. However, the maximum von Mises stresses in the bone, implant, and screws for the three static pelvic conditions were increased linearly, and the difference of each part decreased with an increase in the pre-stress.

However, the pre-stress cannot be increased indefinitely, and is constrained by the strength of the structure. In these three static positions, when the pre-stress is below 2000 N, the maximum von Mises stress of the RP is 614.6 MPa, lower than the yield strength of Ti-6Al-4V alloy (789 MPa – 1013 MPa)[23], which indicated the strength of the designed prosthesis can sustain the static loading requirement. Moreover, given that the implant and screws will be affected by the sustained impact load during its service life, the fatigue strength of the prosthesis should also be guaranteed, and in this case, the maximum stress should be far below the fatigue strength limitation of the titanium alloy (310 MPa – 610 MPa)[24]. For an unhealthy leg stance, the maximum von Mises stress of one screw is 337.2 MPa when the pre-stress is 1000 N (approximately 2.6 N·m). When the pre-stress is increased to 1500 N, there is already a large area of the screw with a stress of greater than 310 MPa (Fig. 8b). Therefore, the pre-stress should not exceed 1000 N during surgery to avoid a fracture from screw fatigue.

It is not always the case that more screws can improve the fixation of a prosthesis, since some screws might bear minimum load. Additionally, more screws mean more traumas and greater risk of infection, which is not ideal for the patient to recover. Therefore, one of the purposes in our manuscript is to reduce the number of screws whilst ensuring the stability of the prosthesis. Therefore, by removing four screws (Fig. 1c) from the original system and calculating the stress of the reconstructed pelvis, comparison shows that the magnitude and distribution of the stresses were basically the same

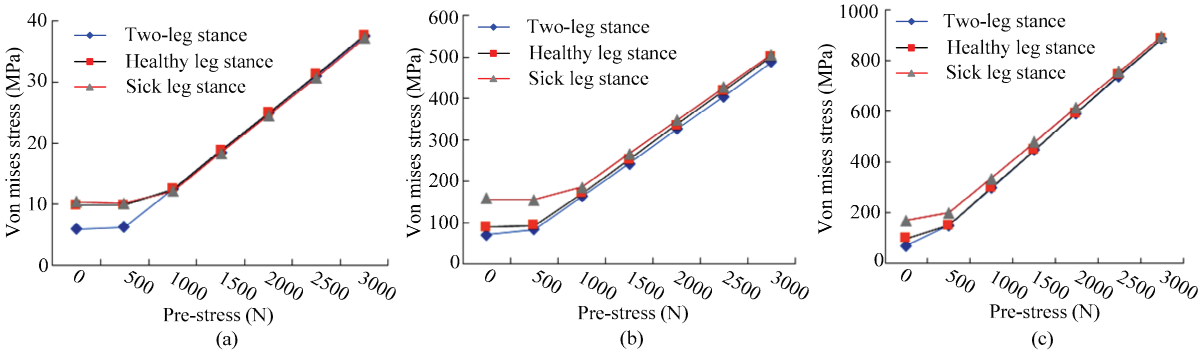

Fig. 6 Maximum stresses in (a) bone, (b) implant, and (c) screws under different pre-stresses (four screws removed).

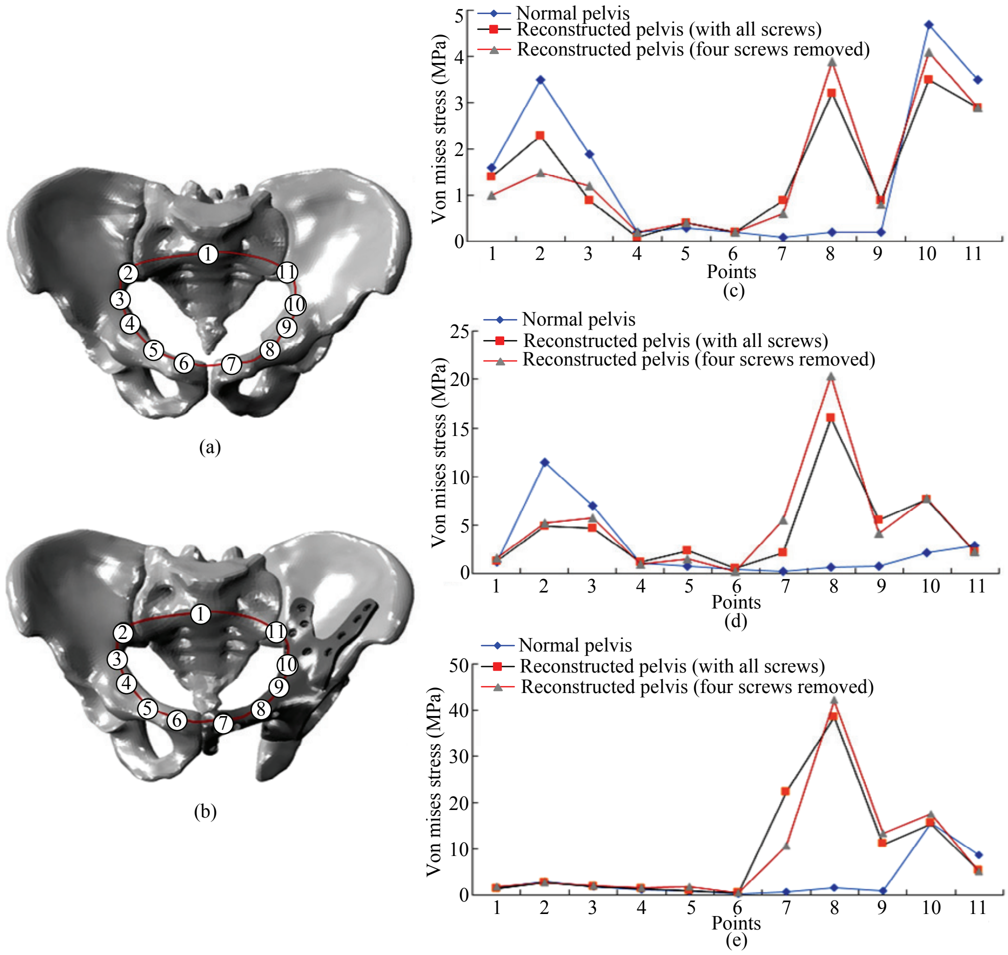

Fig. 7 Selected nodes on pelvic ring of (a) normal and (b) reconstructed pelvises, and the von Mises stresses at the selected nodes during (c) two-leg stance, (d) healthy leg stance, and (e) unhealthy leg stance.

when the same screw pre-stress was applied for both cases. For these two RP models that applying the full number of screws and removing four screws, when the pre-stress is below 3000 N, the difference in maximum von Mises stress in the implant and screws is below 15% and 17%, respectively. Although the maximum stress in the bone is quite different (below 50%), it is still lower than the fatigue strength of the cortical bone (37 MPa – 57 MPa)[25].

As the results shown in Fig. 7, due to the stress shielding, the stresses of the nodes on the implant (nodes 7–10) of the RP were 1.1- to 20-times greater than the

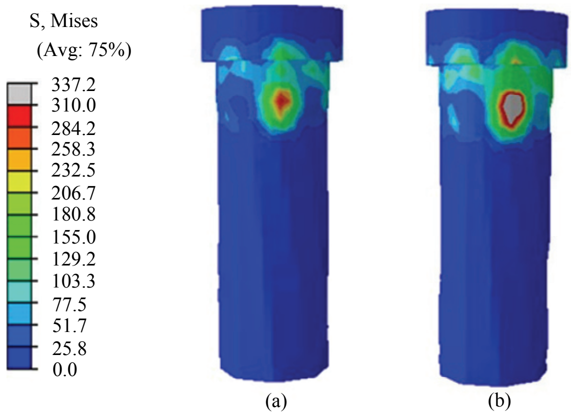

Fig. 8 Von Mises stress distribution of a screw when the pre-stress is (a) 1000 N and (b) 1500 N for an unhealthy leg stance.

stresses of the nodes on the same positions that near the sacroiliac joint and the symphysis pubis regions of NP. However, for the rest of the regions, the stress distribution profiles were similar between NP and RP. Moreover, for the two RP models that applying the full number of screws and removing four screws, the stresses of the selected points were basically the same. Therefore, custom-made prosthesis can restore the load transferring of the pelvis and four screws can be removed during surgery to reduce trauma.

There are certain disadvantages to our work. Previous experimental studies have found that the resultant force acting through the hip joint during normal walking is around 300% the Body Weight (BW)[26], and can reach up to 1000% the body weight when running and jumping[27,28]. Therefore, further studies should investigate the stress on the pelvis during more strenuous activity.

5 Conclusion

Using the FE method, the effects of the pre-stress and fixation type of screws applied on the biomechanics of an RP with a custom-made implant were studied. It can be found that the stress gathers around the screws and the maximum von Mises stress of the RP system is increased with the increase in pre-stress when different pre-stress levels were applied. Pre-stress value was suggested to be set below 1000 N when the fatigue life of the screw was considered. Moreover, on the supposition that the surgeon used too many screws on the alar part of the implant, four screws were removed from the original RP system and the stress of the RP was calculated. Compared to the stress of the RP that all screws applied, the magnitude and distribution of the stresses were basically the same. This indicated that those four screws can be removed without affecting the stability of the prosthesis.

Acknowledgment

This work was supported by the Program of the National Natural Science Foundation of China (Grant Nos. 51205303 and 51323007), the Fundamental Research Funds for the Central Universities, the Research Fund for the Doctoral Program of Higher Education of China (RFDP), and the Program of International Scientific & Technological Cooperation and Exchange Planning of Shaanxi Province (Grant No. 2017KW-ZD-02).

References

[1] Hao Z X, Wan C, Gao X F, Ji T, Wang H S. The effect of screw fixation type on a modular hemi-pelvic prosthesis: A 3-D finite element model. *Disability and Rehabilitation: Assistive Technology*, 2013, **8**, 125–128.

[2] Jia Y W, Cheng L M, Yu G R, Du C F, Yang Z Y, Yu Y, Ding Z Q. A finite element analysis of the pelvic reconstruction using fibular transplantation fixed with four different rod-screw systems after type I resection. *Chinese Medical Journal*, 2008, **121**, 321–326.

[3] Hua Z K, Fan Y W, Cao Q H, Wu X B. Biomechanical study on the novel biomimetic hemi-pelvis prosthesis. *Journal of Bionic Engineering*, 2013, **10**, 506–513.

[4] Wang B, Sun P D, Xie X B, Wu W D, Tu J, Ouyang J, Shen J N. A novel combined hemipelvic endoprosthesis for peri-acetabular tumours involving sacroiliac joint: A finite element study. *International Orthopaedics*, 2015, **39**, 2253–2259.

[5] Zhou Y, Min L, Liu Y, Shi R, Zhang W L, Zhang H, Duan H, Tu C Q. Finite element analysis of the pelvis after modular hemipelvic endoprosthesis reconstruction. *International Orthopaedics*, 2013, **37**, 653–658.

[6] Kitagawa Y, Ek E T, Choong P F M. Pelvic reconstruction using saddle prosthesis following limb salvage operation for periacetabular tumour. *Journal of Orthopaedic Surgery*, 2006, **14**, 155–162.

[7] Cottias P, Jeanrot C, Vinh T S, Tomeo B, Anract P. Complications and functional evaluation of 17 saddle prostheses for resection of periacetabular tumors. *Journal of Surgical Oncology*, 2001, **78**, 90–100.

[8] Mavrogenis A F, Soultanis K, Patapis P, Guerra G, Fabbri N, Ruggieri P, Papagelopoulos P J. Pelvic resections. *Orthopedics*, 2013, **35**, 232–243.

[9] Dai K R, Yan M N, Zhu Z N, Sun Y H. Computer-aided custom-made hemipelvic prosthesis used in extensive pelvic lesions. *The Journal of Arthroplasty*, 2007, **7**, 981–986.

[10] Iqbal T, Shi L, Wang L, Liu Y X, Li D C, Qin M, Jin Z G. Development of finite element model for customized prostheses design for patient with pelvic bone tumor. *Journal of Engineering in Medicine*, 2017, **231**, 525–533.

[11] Colen S, Dalemans A, Schouwenaars A, Mulier M. Outcome of custom-made IMP femoral components of total hip arthroplasty a follow-up of 15 to 22 years. *The Journal of Arthroplasty*, 2014, **29**, 397–400.

[12] Ji T, Guo W, Tang X D, Yang Y. Reconstruction of type II+III pelvic resection with a modular hemipelvic endoprosthesis: A finite element analysis study. *Orthopaedic Surgery*, 2010, **4**, 272–277.

[13] Fan Y P, Lei J Y, Zhu F, Li Z Q, Chen W Y, Liu X M. Biomechanical analysis of the fixation system for T-shaped acetabular fracture. *Computational and Mathematical Methods in Medicine*, 2015, **2015**, 1–10.

[14] Böhme J, Shim V, Höch A, Mütze M, Müller C, Josten C. Clinical implementation of finite element models in pelvic ring surgery for prediction of implant behavior: A case report. *Clinical Biomechanics*, 2012, **27**, 872–878.

[15] Bellini C M, Galbusera F, Ceroni R G, Raimondi M. Loss in mechanical contact of cementless acetabular prostheses due to post-operative weight bearing: A biomechanical model. *Medical Engineering* & *Physics*, 2007, **27**, 175–181.

[16] Er M S, Eroglu M, Verim O, Altinel L. Finite element analysis of the pelvis after modular hemipelvic endoprosthesis reconstruction. *International Orthopaedics*, 2013, **37**, 2097–2098.

[17] Ji T, Gao X F, Guo W. Construction of a three-dimensional finite element model of the pelvic ring. *Journal of Clinical Rehabilitative Tissue Engineering Research*, 2009, **13**, 1625–1628.

[18] Leung A S, Gordon L M, Skrinskas T, Szwedowski T, Whyne C M. Effects of bone density alterations on strain patterns in the pelvis: Application of a finite element model. *Engineering in Medicine*, 2009, **223**, 965–979.

[19] Palastanga N, Soames R W. *Anatomy and Human Movement*: *Structure and Function*, 6th ed., Churchill Livingstone, Edinburgh, UK, 2012.

[20] Andersen R C, O'Toole R V, Nascone J W, Sciadini M F, Frisch H M, Turen C W. Modified stoppa approach for acetabular fractures with anterior and posterior column displacement: Quantification of radiographic reduction and analysis of interobserver variability. *Journal of Orthopaedic Trauma*, 2010, **24**, 271–278.

[21] Hao Z, Wan C, Gao X, Ji T. The effect of boundary condition on the biomechanics of a human pelvic joint under an axial compressive load: A three-dimensional finite element model. *Journal of Biomechanical Engineering*, 2011, **8**, 965–979.

[22] Dalstra M, Huiskes R. Load transfer across the pelvic bone. *Journal of Biomechanics*, 1995, **28**, 715–724.

[23] Hosseini S, Hudak R, Penhaker M, Majernik J. Fatigue of Ti-6Al-4V. *Biomedical Engineering Technical Applications in Medicine*, 2012, **17**, 75–92.

[24] Long M, Rack H J. Titanium alloys in total joint replacement — A materials science perspective. *Biomaterials*, 1998, **19**, 1627–1639.

[25] Zioupos P, Gresle M, Winwood K. Fatigue strength of human cortical bone: Age, physical, and material heterogeneity effects. *Journal of Biomedical Materials Research*, 2008, **86**, 627–636.

[26] Phillips A T M, Pankaj P, Howie C R, Usmani A S, Simpson A H R W. Finite element modelling of the pelvis: Inclusion of muscular and ligamentous boundary conditions. *Medical Engineering* & *Physics*, 2007, **29**, 739–748.

[27] Bergmann G, Deuretzbacher G, Heller M, Graichen F, Rohlmann A, Strauss J, Duda G N. Hip contact forces and gait patterns from routine activities. *Journal of Biomechanics*, 2001, **34**, 859–871.

[28] Bergmann G, Graichen F, Rohlmann A. Hip joint loading during walking and running, measured in two patients. *Journal of Biomechanics*, 1993, **26**, 969–990.